

The Electrostatic Field Networking in Three Isolated Thunderstorms

Zhenhui Wang^{*1, 2,a}, Qingfeng Zeng^{1, 2,b}, Fengxia Guo^{2,c}, Dongpu Xu^{3,d}, Hao Wang^{2,e}

¹Key Laboratory of Meteorological Disaster of Ministry of Education, Nanjing University of Information Science & Technology, Nanjing 210044, P. R. China

²School of Atmospheric Physics, Nanjing University of Information Science & Technology, Nanjing 210044, P. R. China

³Jiangyin Meteorological Bureau, Jiangyin 214400, P. R. China

*corresponding author, e-mail: ^a eiap@nuist.edu.cn, ^b zengqing0419@sina.com, ^c aguo_fx@yahoo.com.cn, ^d xudongpu@hotmail.com, ^e wanghao911@163.com

Abstract

A method for networking atmospheric electrostatic field by a quasi-normal charge distribution model based on radar and sounding data in isolated storm cells has been proposed. The charge distribution parameters of thundercloud are first estimated and inversed, and then the network of atmospheric electrostatic field can be calculated with the obtained parameters. The method was used to analyze three isolated thunderstorms that passed through the experiment site in 2009. It was shown that the electrostatic field networking and the charge distribution were concordant with the location of lightning and radar echo. It is revealed that the model and obtained parameters are reasonable to some extent and the method for networking electrostatic field using radar and sounding data is feasible.

Keywords: *atmospheric electrostatic field networking, Doppler weather radar, isolated storm*

Copyright © 2013 Universitas Ahmad Dahlan. All rights reserved.

1. Introduction

Thunderstorms are one of the major causes of weather-related human injuries, death and tremendous loss of property. With the rapid development of economy and extensive application of electronic technology, lightning hazard traverse many fields, such as agriculture, aviation, infrastructure and telecommunications. Hence the works of lightning monitoring, forecasting and defense have become increasing useful. Lightning activity often causes a significant change of EF near the ground. The EF data can reflect the charges of thundercloud quickly and it is an important parameter used for charge distribution research and lightning forecasting. Scholars (e.g. [1-2]) attempted to utilize the EF data to charge distribution research in thunderclouds. Other scholars made use of the EF thresholds [3, 4], 0-1 relations of curve quick jitter [5] and polarity reversal [4] as methods for lightning nowcasting. Some scholars also tried to forecast lightning by combining EF data with lightning location [6] or radar data [7]. However most of them have used EF data from a single-station. This data can only reflect the charge situation in a small region around the field mill and cannot show the space and time characteristics of a whole thunderstorm. Therefore if EF can be networked, it is possible to enhance the monitoring function and enlarge the detection range of the field mill. The most common method for networking EF is spatial interpolation using limited data. Due to the economic and manpower factors, the site setting of field mills are sparse and discrete in the observation region. There can be some deviation between networked EF with interpolation methods and actual observation data. Since EF data can reflect the charge situation in a thundercloud and the size of the charged thundercloud can be described by radar data, we can try to network the EF data base on the existing charge structure with this data. This work therefore presents an analysis of EF networking using radar and sounding data based on a quasi-normal charge distribution model.

2. Observation mill and data

More than 25 field mills have been installed in Nanjing and its surrounding areas to study the law and characteristic of EF space-time variation. The positions of the EF mill together with Nanjing new generation Doppler weather radar station are shown in Fig.1. The dot in Fig. 1 is Nanjing weather radar, its scan time is 6minutes and the detection range is 230km. The observation area is located in a low-lying plain and a thunderstorm prone area known as the Yangtze River Delta.

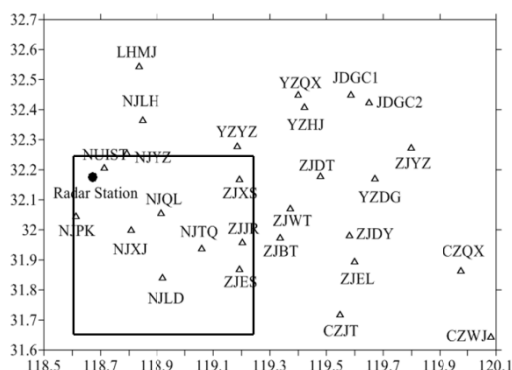


Figure 1. Location of EF and radar stations in experiment site.

The EF meters are of two kinds; balloon-born two spheres and the field mill. The field mill electric field meter (it is written as field mill in the paper) was used in this paper. The field mill measures EF changes through a windmill-type detection probe. First, the induced charge of stator which is produced by the rotation of a moving film is converted into voltage that is proportional to EF. The EF value can consequently be calculated by measuring this voltage on the stator. The alternating current signal on the sensor chip is very weak reaching a value of 10^{-11} - 10^{-12} V and hence it is amplified by I-V conversion circuit and changed into AC voltage signal. The AC voltage signals as well as the synchronizing signals produced by photoelectric switch are sent to a phase sensitive detector and the polarity of the EF is identified using this detection. At last the voltage signal which is up the requirement of analog-to-digital converter is obtained after going through low-pass filtering, voltage regulation and the offset circuit.

The amplification is linear hence the relation between voltage signal U and electric field E is as follows: $U=kE$, where k is a constant. The field mill basic calibration principle is done using the relation between voltage and electric field $U = Ed$ (d is the distance between the two plates). First, some voltage is added on two parallel plates and from the formula the EF intensity between the two plates is known. Based on this principle, the device is put in two plates and the potentiometer is adjusted until the output of the electric field device and simulation of electric field is the same. The EF data is packaged into a frame and each frame of data consists of ordinal, measured values, acquisition time, motor speed and check codes. After the installation of field mills, data is transmitted through a wireless connection to a receiver and the data is finally stored simultaneously on two computers.

The EF is defined here as the negative charge if the charge of the cloud is positive and vice versa. Depending on the magnitude and location of charge, the cloud field could be detected in a range close to 20 km and its response time is 1 s. To weaken the environmental effect on EF measurements two ideas are used. First, The EF mill at latitude [31.85-32.20N] and longitude [118.60-119.25E], which installed in standard meteorological observatories and situated in an open and flat field with no high objects around them, has been selected in this paper. Secondly, the EF was unified and identified on 0.13kV/m [8] based on the fair-weather which is restricted by global and local daily variation mechanism and the mean values occur in a consistent pattern [9, 10]. Besides, the rationality of calibrated data are also measured and compared, and the results show that the standard deviation of 8 stations is small. The resolution of field mill is about 1V/m and the accuracy of EF is enough for the networking work.

3. Methodology descriptions

The charge in the thunderstorm can be reflect by EF data, while the size of the charged thundercloud can be described by radar data, therefore the main charge parameters of thundercloud can be obtained based on EF, radar, sounding and the other information through the model, and then the space EF can be recalculated and networked according to these obtained charge parameters.

3.1. Quasi-normal charge distribution model

In practice, some meteorological elements, such as temperature and precipitation, have the feature in some frequency distribution, i.e., the frequency is greatest in its average and the frequency of both sides will decrease gradually. So many factors, such as environmental temperature, particle moving speed, particle size, friction rates and the effect of coagulation, collision, hydrometeors in different phases (such as liquid, crystal, snow and graupel), will make a different contribution to the production and distribution of charges. In addition, the transfer from positive ions to negative and vice versa in electrification process is stochastic. Therefore, it is quite difficult to describe the charge distribution in a thundercloud. The charge distribution of thunderclouds is taken as the results produced by a numbers of "random" factors hence it is described with normal or quasi-normal function in this study. The charge distribution of a single-polar charged mass in terms of Gaussian function can be expressed as:

$$\rho(x, y, z) = \rho_0 \exp\left[-\frac{1}{2}\left(\left(\frac{x-x_0}{\sigma_x}\right)^2 + \left(\frac{y-y_0}{\sigma_y}\right)^2 + \left(\frac{z-z_0}{\sigma_z}\right)^2\right)\right] \quad (1)$$

Where A (x_0, y_0, z_0) is charge concentration center of charged mass, ρ_0 is the charge density at this point and $\sigma_x, \sigma_y, \sigma_z$ are parameters for the charge density that decrease with distance from the center, which is similar to the standard deviation in Gaussian function.

According to the knowledge of physics, because of the balance effect of total electric field, the induced charge will appear on the ground when a thunderstorm occurrence. The electric field near the ground is the joint function of the charge in the cloud and on the ground. The electric field measured near the ground is electrostatic field and can be described by Coulomb law and mirror image. The EF intensity at point (x, y, z) around the single-polar charged cloud would be

$$\vec{E}(x, y, z) = \frac{\rho_0}{4\epsilon} \left[\int_{x_0-\Delta x/2}^{x_0+\Delta x/2} \int_{y_0-\Delta y/2}^{y_0+\Delta y/2} \int_{z_0-\Delta z/2}^{z_0+\Delta z/2} \frac{\vec{r} \exp\left[-\frac{1}{2}\left(\left(\frac{x'-x_0}{\sigma_x}\right)^2 + \left(\frac{y'-y_0}{\sigma_y}\right)^2 + \left(\frac{z'-z_0}{\sigma_z}\right)^2\right)\right]}{\left[\sqrt{(x-x')^2 + (y-y')^2 + (z-z')^2}\right]^3} - \vec{r} \exp\left[-\frac{1}{2}\left(\left(\frac{x'-x_0}{\sigma_x}\right)^2 + \left(\frac{y'-y_0}{\sigma_y}\right)^2 + \left(\frac{z'-z_0}{\sigma_z}\right)^2\right)\right]}{\left[\sqrt{(x-x')^2 + (y-y')^2 + (z+z')^2}\right]^3} \right] dk' dy' dz' \quad (2)$$

Where $\vec{r} = [(x-x'), (y-y'), (z-z')]$, ϵ is an atmospheric dielectric constant and parameters $\Delta x, \Delta y, \Delta z$ are the limits for integration calculation which stand for the 3-dimensional size of the charged mass and is estimated from the radar echoes of the thundercloud. The position of charge density center A (x_0, y_0, z_0) and charge distribution parameters $(\sigma_x, \sigma_y, \sigma_z)$ are also estimated according to the radar echo features of cloud.

When a charged cloud move with a certain speed to a mill station, the EF at this station would change with time and can be calculated using Eq. (2) by ignoring the short time variations of charge in the mature, stable thundercloud. In the meantime, Eq. (2) can be used for calculating the EF caused by a cloud with multi-polar charge structure after modification.

The charge structure of thundercloud is not single-polar but complicated (multi-polar) in practice, and it is necessary to use some charge structure in the inversion of charge parameters. Krehbiel [11] found that although the heights of the main negative charge region were different in three different areas, they were in the same temperature zone. Although the charge structure of thundercloud is complex, the main charge structure can describe as dipole or tripole in the main charge area [12-15] in a mature convection zone. The numerical results [16] of three regions in China and [17] in Chinese plateau region also confirmed this conclusion and found that the charge structure can be described as dipole or tripole charge structure in mature stage. The charge structure research in Nanjing is few and there are no other means to

detect directly. The simple tripole structure is used in this model, i.e. the upper positive, the central negative and the lower positive charge (if the lower positive charge is less or zero, it become dipole structure). The rationality of results will be verified by the independent EF data, lightning location data and the inversion charge density.

3.2. EF networking

It is shown from Eq. (2) that if the discharge distribution (function Eq. (1)) and the sizes feature of thundercloud is known, the space EF distribution near ground can be calculated with the model. As mentioned above, the parameters $\Delta x, \Delta y, \Delta z, x_0, y_0, z_0, \sigma_x, \sigma_y, \sigma_z$ can be estimated from the different types of data. The EF data is obtained by observation and therefore only parameters ρ_0 of the three layers are unknown. This can be calculated from three or more than three EF values. The parameters of charge density is inverted as follows, first, the EF values of different layers in simple tripole structure of inversion stations are calculated with the charge density of $1\text{C}/\text{km}^3$ and then the reasonable charge density range ($0\text{-}30\text{C}/\text{km}^3$) and step ($0.001\text{C}/\text{km}^3$) of each layers are set to be composed of different charge density combinations. Finally the total error percentage and standard deviation between simulated and observed EF of inversion stations under different charge density combinations are calculated circularly using the least square method. The smallest error percentage of charge density combinations is considered as optimum. If the error percentage between simulated and observed EF which is greater than 100% reach 60% in 6 min, the parameters $\sigma_x, \sigma_y, \sigma_z, x_0, y_0$ and z_0 will be adjusted and simulated again. To verify the simulation parameters obtained, the EF of other station are simulated with the model and the obtained parameters and compared with the observation data. After a different adjustment, if there are no parameters satisfying the above requirement or the error between test results and observations is too large, this simulation of the stage is considered as a failure. If the EF parameters is inverted successfully, the EF networking near ground will be recalculated. When the observation sites are adequate, time synchronization data of different sites are used in the solution otherwise the data obtained at different time intervals from the same site are used.

4. Case analysis and results

The isolated storm cells of July 15 (20090715), August 14 (20090814) and August 24 (20090824) in 2009 which passed through the research regions were analyzed. The EF measurement may be affected by charged precipitation and hence may not reflect the charge of the thundercloud. Therefore the EF data under strong radar echo is not included in the process of inversion and interpolation. For instance, NJXJ station which was covered by radar echo was excluded in the case of 20090814. The slow EF variations (300s average value) of time synchronization data in different sites was used in the 20090814 and 20090824 case, while the data from different time intervals in the same site was used in the 20090715 case. The variations of charge distribution in the time interval of 10s is ignored, i.e., a charge density combination is calculated every 10s. Because of the simple tripole structure used in the model, the isolated cells and the closed stage of the radar-echo tightly are analyzed and networked in this paper.

4.1. The case of 20090814

A thunderstorm occurred and developed around NJXJ station at about 0748 UTC August 14, 2009. There were 8 synchronized EF observation stations (NUIST, NJQL, NJXJ, NJTQ, ZJJR, NJJP, NJSH and ZJEL) at the experiment site. To avoid the effect of precipitation, NJXJ station which was covered by radar echo was excluded when inversion and networking. The EF observation of NJQL, NJTQ and NJLD was the inversion data, while NJPK was independent test data in this case. Before inversion, first, with NJXJ station as the origin and the increase in the directions of longitude and latitude as X, Y axis separately, the coordination system was built up, and then the information of latitude and longitude, such as the site as well as the thunderstorm cloud path were converted into Cartesian coordinates.

4.1.1. Parameter selection

Taking into account the charge structure research [18,19], the numerical simulation results [16] in China as well as the Chinese inland sounding experiments [17], this study selected the region below -5 dBZ as the lower positive charge region of thunderstorm and the center was about 0 dBZ; the region -5 dBZ ~ -20 dBZ as the negative charge region and the center height was about -10 dBZ; the region -20 dBZ ~ -40 dBZ as upper positive charge region and the center height was about -30 dBZ. Ambient temperature height which the study required was estimated based on the corresponding sounding data. Taking the process of 0812 UTC as an example to explain how to determine the parameters of the model required.

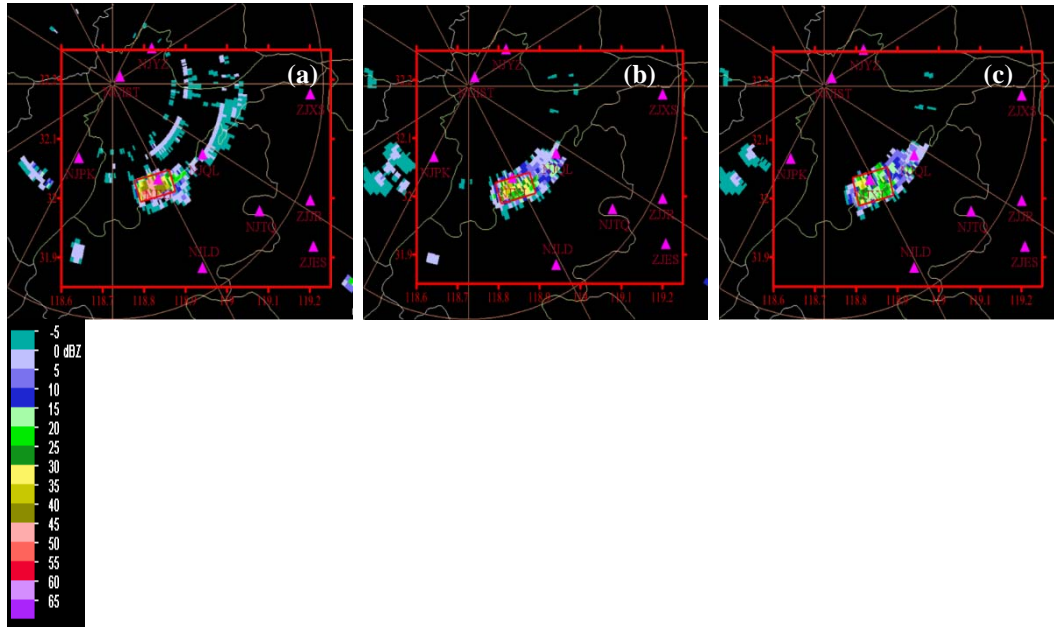


Figure 2. The radar CAPPI at 0812 UTC on August 14, 2009. (a) 5km; (b) 7km; (c) 9km.

According to the sounding data, the radar CAPPI (Constant Altitude Plan Position Indicating) of 5, 7, 9 km can well represent the radar echo of lower, central and upper respectively. Fig.2 is showing the radar CAPPI of 5, 7, 9 km at 0812 UTC on August 14, 2009. The distributions of stations in Fig.2 are consistent with Fig.1 and the box around the echo is echo centralized area. The parameters x_0 , y_0 , Δx and Δy of different layers were determined by the center and the scale of echo centralized area (greater than 25 dBZ in lower charge region; greater than 15 dBZ in upper and central region) of corresponding height CAPPI respectively. The integration-limits parameter Δz of lower positive charge region were determined by the echo thickness which the echo was greater than 25dBZ below 6.5km (environmental temperature was about -5°C). The parameter Δz of lower positive charge region was about 4.5km. The integration limits parameter Δz of central and upper charge region were determined by radar echo and sounding temperature profile. The parameter Δz of central negative charge region (-5°C ~ -20°C) was about 2.5km while upper positive charge region (-20°C ~ -40°C) was about 3km. The parameters σ_x , σ_y were determined by the scale of echo centralized area which was greater than 30 dBZ (lower charge region) or 20 dBZ (upper and central region). As for the parameter σ_z , many researches [14,15,17,20] pointed out that it ranged from hundreds of meters to 2km. The parameter σ_z of upper and central region was valued 1.5km in this paper. The parameter σ_z of lower positive charge region was determined by echo thickness that the echo was greater than 35dBZ below 6.5km, and it was about 3.5km. In addition, the echo thickness in the simulation process changed little, so the parameters z_0 , σ_z , Δz were considered to be the

same. The parameter z_0 of different layers was the central height of these layers and determined by the Nanjing station sounding temperature profile. Meanwhile, the parameters Δx , Δy , σ_x , σ_y in the adjacent radar scan time is considered to be changed linearly in inversion calculation.

4.1.2. The simulated results and contrast analysis

The thunderstorm process between 0812-0830 UTC was simulated and the results are shown in fig 3. The stations of NJQL, NJTQ and NJLD were inversion data, and the measured and simulated EF are in fig 3a,b. The NJPK was independent test station, and the measured and simulated EF values were shown in Fig 3a. The simulated EF of test station was calculated with the model and the obtained parameters. The coefficient of NJPK station between measured and simulated EF was 0.86. The inversion and independent test EF all indicated that the observations and simulated EF were in good agreement. It was speculated that the model and the obtained parameters were rational to some extent. Fig 3c is the evolution of charge center density of this case. It was exhibited that the negative charge density of central region had the largest value while positive charge density of lower and upper were small relatively. Especially, the positive charge density of lower layer was small (most of them were zero) before 0824 UTC and the structure was dipole at this stage, which corresponded with the development of thunderstorm; After 0824 UTC the charge density of lower layer increased gradually and the structure assumed a tripole charge structure, which corresponded with the matured stage of thunderstorm. Meanwhile, lightning location data indicated that the two negative flashes occurred at about 0825 UTC (the erect dotted line in the Fig 3c and the measured EF in Fig 3a,b). The charge structure was tripole when CG lightning occurred. The EF networking characteristics of 0818 and 0825 UTC of different charge structure of thunderstorm respectively were analyzed in this paper.

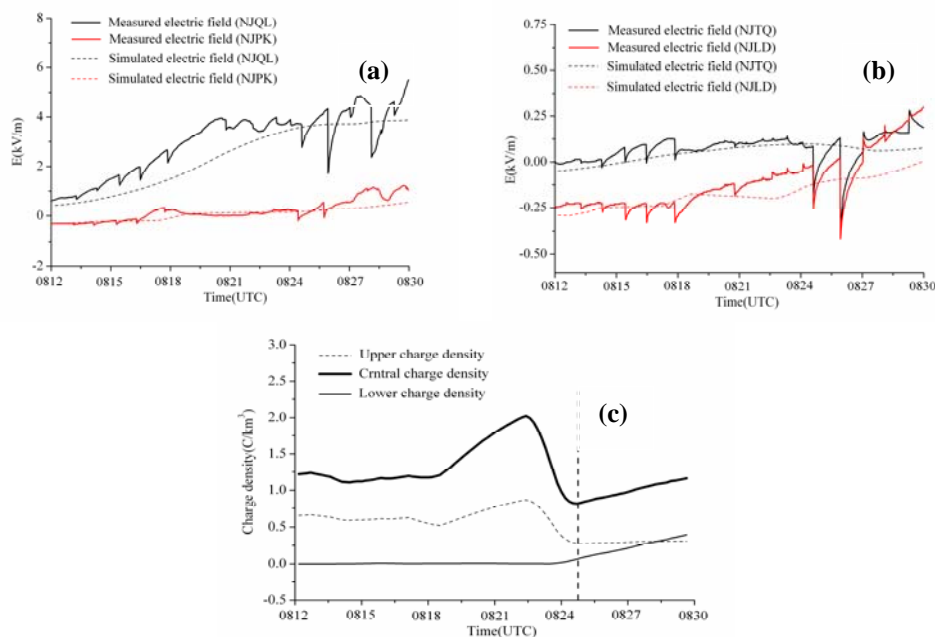


Figure 3. Measured and simulated EF and charge distribution on August 14, 2009. (a) Measured and simulated EF of NJQL and NJPK; (b) Measured and simulated EF of NJLD and NJTQ; (c) The charge evolution on August 14, 2009. The charge density is absolute value.

Figure 4a and b are showing the values of EF networking which were obtained by calculating with the model at 0818 and 0825 UTC respectively. The radar echo in this figure is radar PPI (plan position indicating) at 14.6° elevation (the same below). There were no CG

lightning occurred at 0818 UTC and Figure 3 showed that the charge structure of thundercloud was dipole. Because the charge structure was dipole as well as the negative cloud charge of central layer was large, the EF in radar echo surrounding area had a large positive value, such as Figure 4a. The LLS disclosed that there were two negative CG lightning flashes occurred at 0825 UTC. In the meantime, Figure 3c showed that the charge structure changed from dipole at 0818 UTC to tripolar before the lightning happened. Except for the positive EF region similar to 0818 UTC, there appeared a negative EF area around the radar echo center which was resulted from the positive charges in lower part of the thundercloud, as shown in Figure 4b,c. Figure 4c is the space-distribution of EF network at 0825 UTC, which can exhibit the EF distribution visually. It is exhibited that the positive charge area was small and therefore the negative EF region was also small. Figure 4d shows the charge density of different layers in thundercloud when the lightning occurred, the filled contour map in color is negative charge density of central layer, the red and black contours were positive charge density of lower and upper layer. The charge density distribution in figure was compared with radar echo and it was found that the charge center density was coincident with the radar echo. It also showed that the CG lightning occurred at the place between the center of negative charge in central layer and positive charge in lower layer, which indicated that location of lightning was in accordance with charge center density.

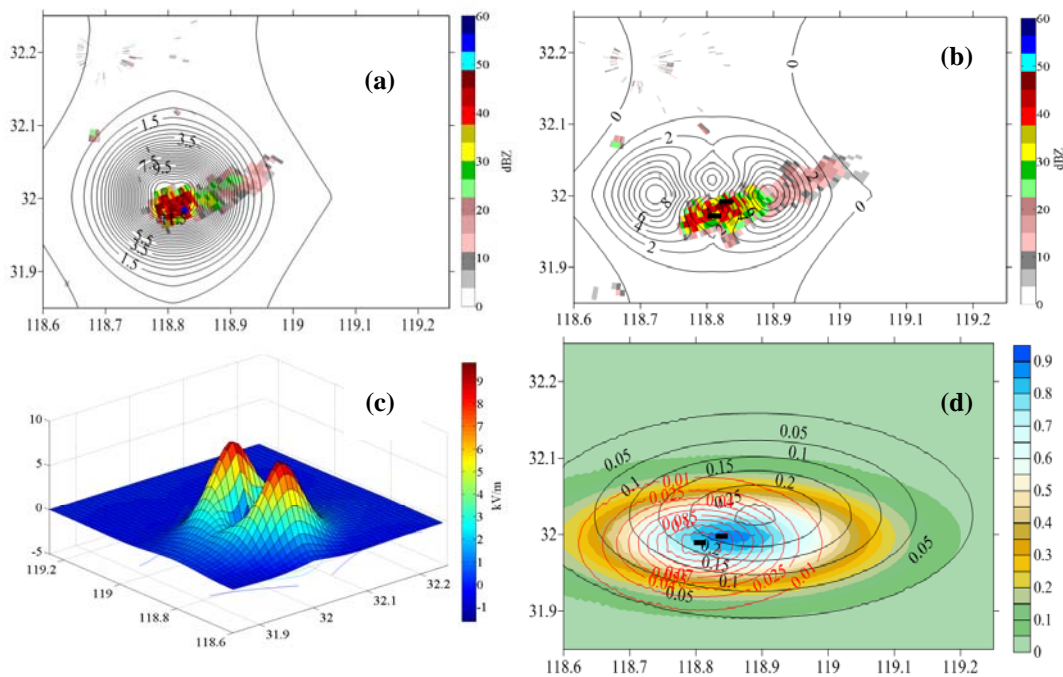


Figure 4. The EF networking in the case of 20090814.(a) The EF networking with model at 0818 UTC; (b) The EF networking with model at 0825 UTC; (c) The EF distribution at 0825 UTC;(d)The charge distribution at 0825 UTC. The charge density is absolute value.

4.2. The case of 20090824 and 20090715

Using the same method as used in the case 20090814, the case 20090824 was reversed with data of time synchronization of different sites (NJXJ, XJLD, NJTQ were used as inversion data and NJQL was used as test data), while 20090715 was reversed with data of different times of the same site (this thundercloud was beside NJXJ and NJLD station, therefore NJXJ was used as an inversion data and XJLD was used as test data). The evolution of charge center density in different layers of the two cases is shown in figure 5a & b. The simulated and measured EF values of inversion and test were similar to the case of 20090814. Combined with the radar data of the two cases, it was found that the evolution of charge center density was similar to the case of 20090814 and the charge structure evaluated like this: the charge

structure of thundercloud in development phase was dipole, the matured stage was tripole and it became dipole when the thundercloud was extinct. The charge density evolution of case 20090824 is shown in figure 5a and the erect dotted line about 0718 UTC is the beginning of lightning occurred while the erect dotted line about 0736 UTC is the end of lightning. There occurred 15 lightning flashes during this stage and fig.5a indicated that the charge structure during the occurrence of lightning was tripole. Fig 5b is the center charge density evolution of 20090715 and there was one lightning occurred (the place at the erect dotted line) in this case. The same as in the cases of 20090824 and 20090814, the lightning charge structure was also tripole when the lightning occurred. Figure 5c & d are showing the EF network of 20090824 and 20090715 when lightning occurred respectively. The networked EF was simulated according to the model. It is indicated that the EF network and the radar echo were in good agreement. Meantime, because of the existence of positive charge in the lower layer, there was a small negative EF area beneath the strong radar echo, which were similar to the case of 20090814. Meanwhile, the location of lighting occurred and charge density distribution were also in good agreement, which was also the same as that in the case of 20090814.

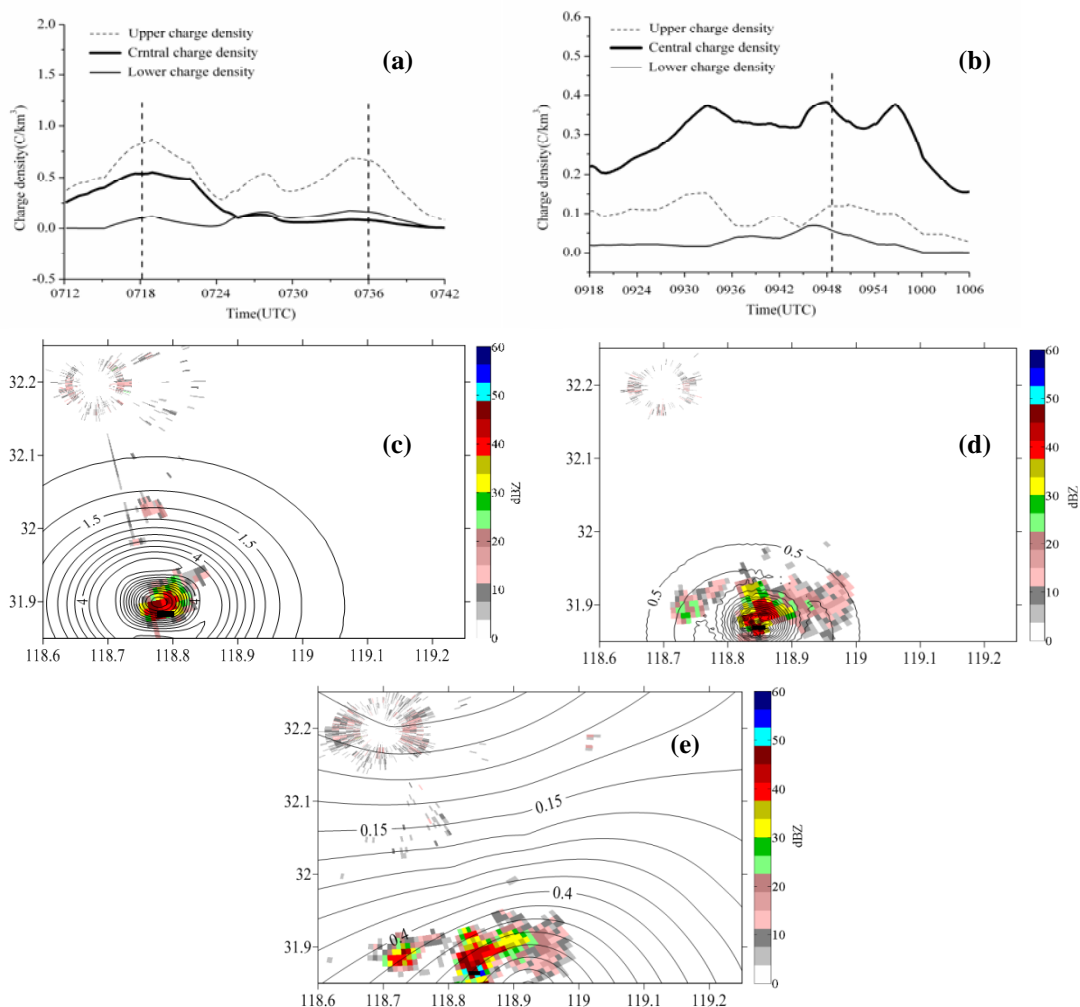


Figure 5. Charge and EF networking distribution in the case of 20090824 and 20090715. (a) Charge evolution in case of 20090824; (b) Charge evolution in case of 20090715; (c) The EF networking with model at 0718 UTC in case of 20090824; (d) The EF networking with model at 0825 UTC in case of 20090715; (e) The EF networking with Kriging interpolation method at 0825 UTC in case of 20090715.

The surface electric field distribution in experimental site can be obtained through limited observation data with space interpolation method. Fig 5e is the EF network at 0825 UTC in the case 20090715 based on the Kriging interpolation method. It was shown that there existed some deviation between model EF network with the location of lightning and radar echo. Meantime, the same result was received in other thunderstorms and with other interpolation methods. So we speculated that it was resulted due to the inadequate intensive site data.

From the analysis of three cases, it was shown that the EF networking and the charge density distribution which obtained from radar and sounding data in isolated storm cells were in agreement with the location of radar echoes and lightning. Meanwhile, the charge structures of three thunderstorms were similar, i.e., the charge structure was dipole in the development, tripole in the mature stage and dipole after matured stage. It was also in coincidence with the fact that the three thunderstorms were of the same type. The charge structure of different stages in thundercloud also shows that the charge structure of thundercloud is complicated. It was also found that the evolution of radar echo and the charge structure in three thunderclouds were basically consistent to the results of researches [21] about strong updraft, electrification activity and EF. Meanwhile, the lightning occurred in the tripole stage in three thunderclouds and the lightning location was between the center of positive charge density in lower layer and negative charge in central layer, which we conjectured that the existence of positive charge in the lower layer of thundercloud may be easier to be excited the CG lightning, because the majority of CG lightning flash began with negative leader and the existence of strong EF area caused by the lower part of thundercloud can easily be excited the leader and the spread to the ground. This result conformed to the conclusion about lightning flashes and lower positive charge [22].

5. Conclusion

With the help of the model, EF data and the relation of radar reflectivity, thunderstorm initial feature, firstly the environmental temperature and charge distribution are implemented in the inversion of charge distribution parameters, and then the EF networking can be calculated with the model and the parameters obtained. Three thunderstorms observed at the site of experiment covered by radar and field mills were analyzed in this paper. The results show that:

- (1) There exists some deviation between the networked EF received from Kriging interpolation method and the location of lightning and radar echo. We conjecture that it is resulted from the sparse data of EF. It illustrates the importance of the layout of EF mill as well.
- (2) The EF networking and the charge density which are obtained by the quasi-normal distribution model is in accordance with the location of the radar echo and CG lighting, which indicated the rationality of the model and parameters to some extent. It is revealed that the method of networked EF using radar and sounding data is feasible.
- (3) The charge structure and charge distribution of different stages in these cases have some indication and reference function for the researches about the characteristics of electricity and lightning forecasting.

Because of the absence of effective means, such as sounding EF to detect the charge structure, the classic charge structure is used in model and at the same time only isolated storm cells are analyzed in this paper. Further study is needed to make the inversion process more objective so that the retrievals would be more reliable and unique. The shielding effect of cloud boundary and the discharge of lightning which brings some errors to results are ignored. These deficiencies will be considered in the future study. Meanwhile, the EF networking with multi-polar (more than tripole) model as well as multi-polar thunderstorm will be carried out under permission of study conditions.

Acknowledgements

We acknowledge Professor Qilin Zhang and Wen'an Xiao, and our friend Muhammad Hasan Ali baig and James Wanjohi Nyaga for their valuable contribution in this research work. The work is supported by China Commonweal Industry Research Project (GYHY200806014) and Program for Postgraduates Research Innovation of Jiangsu Higher Education Institutions (CXLX11_0624).

References

- [1] Liu Q, Guo CM, Wang CW, Yan MH. *The surface electrostatic field-change produced by lightning flashes and the lower positive charge layer of the thunderstorm*. *Acta Meteorologica Sinica*.1987; 45: 500-504.
- [2] Zhao Y, Zhang YJ, Dong DS, Zhang HF, Chen CP, Zhang T. Preliminary analysis of characteristics of lightning in the Nagqu area of the Qinghai-Xizang plateau. *Chinese Journal of Geophysics*. 2004; 47: 405-410.
- [3] Liu CQ, Hou JX, Liu K. Thunderstorm warning and forecast with atmosphere electric field data. *Ningxia Engineering Technology*. 2010; 9: 202-205.
- [4] Aranguren D, Montanya J, Sola G, March V, Romero D, Torres H. On the lightning hazard warning using electrostatic field: Analysis of summer thunderstorms in Spain. *Journal of Electrostatics*. 2009; 67: 507-512.
- [5] Chai R, Wang ZH, Xiao WN, Yang ZJ, Zhang HL, Zhang WB. Application of atmospheric electric field data in lightning warning. *Meteorological Science and Technology*. 2009; 37: 724-728.
- [6] Meng Q, Lv WT, Yao W, He P, Zhang YJ, Liu Q, Li L, Zhang M, Chang C. Application of detection data from electric field meter on ground to lightning warning technique. *Meteorological Monthly*. 2005; 9: 30-33.
- [7] Gao TC, Huang ZY, Zhang P, Yang B. Method of amalgamate atmospheric electric field data and radar data. *Journal of PLA University of Science and Technology*. 2006; 3: 302-306.
- [8] Montanya J, Bergas J, Hermoso B. Electric field measurements at ground level as a basis for lightning hazard warning. *Journal of Electrostatics*.2004; 60: 241-246.
- [9] Chen WM. 2003. Principles of lightning science. *China Meteorological Press*, Beijing.
- [10] Golde R H. *Lightning*, Vol. 1, *Academic Press*, London.1977.
- [11] Krehbiel PR. *The electrical structure of thunderstorms, in the earth's electrical environment*. National Academy Press, Washington, D.C. 1986; 90-113.
- [12] Williams E. The tripole structure of thunderstorms. *Journal of Geophysical Research*.1989; 94: 13151-13167.
- [13] Stolzenburg M. An observational study of electrical structure in convective regions of Mesoscale convective systems. *Ph D diss, University of Oklahoma*, Norman.1996.
- [14] Stolzenburg M, Rust WD, Marshall TC. Electrical structure in thunderstorm convective regions.1. Mesoscale convective systems. *Journal of Geophysical Research*. 1998; 103: 14059-14078.
- [15] Stolzenburg M, Rust WD, Marshall TC. Electrical structure in thunderstorm convective regions. 2. Isolated storms. *Journal of Geophysical Research*. 1998; 103: 14079-14096.
- [16] Zhang, YJ, Yan MH, Zhang, CH, Liu QS. Simulating calculation of charge structure in thunderstorm for different areas. *Acta Meteorologica Sinica*. 2000; 58: 617-627.
- [17] Zhao ZK, Qie XS, Zhang TL, Zhang T, Zhang HF, Wang Y, Yu Y, Sun BL, Wang HB. Electric field soundings and the charge structure within an isolated thunderstorm. *Chinese Sci Bull*. 2009; 54: 3532-3536.
- [18] Workman EJ, Holzer RE. A preliminary investigation of the electrical structure of thunderstorms. *National Advisory Committee for Aeronautics*.1942; 850: 1-29.
- [19] Krehbiel PR, Brook M, McCrocy RA. An analysis of the charge structure of lightning discharges to ground. *Journal of Geophysical Research*. 1979; 84: 2432-2456.
- [20] Marshall T C, Rust W D. Electric field soundings through thunderstorms. *Journal of Geophysical Research*.1991; 96: 22297-22306.
- [21] Guo FX, Zhang YJ, Yan MH. A numerical study of the charge structure in thunderstorm in Nagqu area of the Qinghai-Xizang plateau. *Chinese Journal of Atmospheric Sciences*. 2007; 31:28-36.
- [22] Shao XM, Liu XS. A preliminary analysis of intracloud lightning flashes and lower positive charge of thundercloud. *Plateau meteorology*. 1987; 6: 318-325.